AIChE

Internal Model Control Design for Input-Constrained Multivariable Processes

Ambrose A. Adegbege and William P. Heath
Control Systems Centre, School of Electrical and Electronic Engineering, University of Manchester, Manchester M13 9PL, UK

DOI 10.1002/aic.12540
Published online April 5, 2011 in Wiley Online Library (wileyonlinelibrary.com).

Multivariable plants under input constraints such as actuator saturation are liable to performance deterioration due to control windup and directionality change. A two-stage internal model control (IMC) antiwindup design for open loop stable plants is presented. The design is based on the solution of two low-order quadratic programs at each time step, which addresses both transient and steady-state behaviors of the system. For analyzing the robust stability of such systems against any infinity-norm bounded uncertainty, stability test have also been developed. In particular, we note that the controller input-output mappings satisfy certain integral quadratic constraints. Simulated examples show that the two-stage IMC has superior performance when compared with other existing optimization-based antiwindup methods. The stability test is illustrated for a plant with left matrix fraction uncertainty. A scenario where the proposed two-stage IMC competes favorably with a long prediction horizon model predictive control is described. © 2011 American Institute of Chemical Engineers *AIChE J,* 57: 3459–3472, 2011
Keywords: antiwindup, directionality, internal model control, model predictive control, input constraints, quadratic program

Introduction

Control design for processes under input constraints such as actuator saturation nonlinearities has been widely studied either from a antiwindup design approach[1–6] or from a model predictive control (MPC) perspective.[7–10] For multivariable or multi-input multioutput (MIMO) systems, the presence of control input saturation introduces additional problems due to directional change in control action also known as process directionality[11] alongside the widely known controller windup phenomenon. These two problems, control windup and process directionality, can result in substantial closed-loop performance degradation if not separately accounted for during the controller design.[12]

Correspondence concerning this article should be addressed to A. A. Adegbege at adegbege@yahoo.co.uk.

One class of strongly directional multivariable systems that have received extensive treatments in chemical engineering literatures (e.g. Refs. 1,13–17) are the ill-conditioned systems (those having large condition numbers or with gains that depend on both the input directions and the magnitudes). Such class of systems are known to exhibit high sensitivities to model uncertainties and input nonlinearities/uncertainties.[16,17]

MPC algorithms[7,10] are known to handle such problems associated with control input saturations in multivariable plants. However, robust MPC design techniques increase the controller computational burden enormously and often result in very conservative solutions or even infeasible control problem.[18]

In the design of analytical dynamic controllers such as internal model control (IMC), a common approach is to first design a linear controller neglecting the saturation and then a saturation compensation scheme is added to provide a

graceful closed-loop performance degradation in the presence of saturation.[1] This ad hoc saturation compensation scheme is termed as ''antiwindup''. A specific example of antiwindup design is the modified IMC structure that may be interpreted as solving instantaneously an optimization problem at each time step.[2]

Antiwindup designs must be augmented with dynamic compensators to account for process directionality in MIMO systems. One approach is to scale down all the control inputs in such a way that the control input direction is maintained.[1,12] This approach has been shown to be particularly beneficial to the control of ill-conditioned systems but may not necessarily be optimal.[1] Other optimization based schemes have been suggested.[11,19–22] Some of these incorporate explicit solution of an online optimization at each time step. With modern processes, such online optimization can readily be implemented.[23] This approach is described in this article. One major drawback to some of the existing optimizing antiwindup schemes (e.g Refs. 11, 20–21) is that while they offer optimal dynamic behavior, their performances deteriorate significantly in steady state especially when the constraints are active. Schemes that guarantee optimal steady-state behavior (e.g., Ref. 24) may have poor transient characteristics.

The focus of this study is on an IMC antiwindup scheme that optimizes the transient performance of the system and also guarantees steady-state optimal behavior. We consider a general case where the plant is subject to infinity-norm-bounded model uncertainty. We note that in this case, both the plant uncertainty and the nonlinearity satisfy a certain class of Integral quadratic constraints (IQC), and, therefore, sufficient conditions can be developed for analyzing robust stability of the stability of the constrained closed-loop system. In particular, the unconstrained case reduces to the conventional IMC structure where the robust stability is guaranteed by the small-gain theorem.

This article is structured as follows. The Problem setup section describes the problem set-up and some notations. We introduce the concept of IMC for multivariable antiwindup design in The IMC Antiwindup section. The first contribution of the article is presented in the section entitled Two-State Multivariable IMC Antiwindup Structure, where we present the two-stage IMC antiwindup for not only dealing with the performance degradation associated with control windup and directionality but also for ensuring steady state performance in input constrained multivariable problem. In terms of nominal performance, the two-stage IMC compares favorably with a long prediction horizon MPC while its computational requirement is equivalent to that of a single-horizon MPC. The performance of the proposed approach is illustrated via two simulation examples involving ill-conditioned plants. The second contribution of the article is presented in the section entitled Stability Analysis, where sufficient robust stability tests are constructed for the two-stage IMC antiwindup based on IQC theory. We illustrate the stability test with a simulation example. The plant model has a left matrix fraction uncertainty as well as a control input nonlinearity.

Problem Setup

We consider a class of stable and linear systems described by

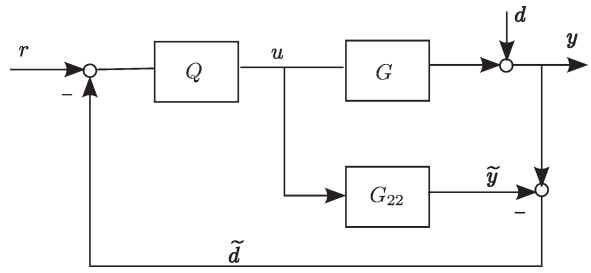

Figure 1. The standard IMC structure.

$$\boldsymbol{y} = \boldsymbol{G}\boldsymbol{u} + \boldsymbol{d} \tag{1}$$

where $\boldsymbol{G}$ is a rational, strictly proper transfer function matrix, and $\boldsymbol{y}, \boldsymbol{d} \in \mathcal{L}^p$, $\boldsymbol{u} \in \mathcal{L}^m$ (or $y, \boldsymbol{d} \in l^p$, $\boldsymbol{u} \in l^m$) are the Laplace transforms (or discrete equivalent, Z-transforms) of the output signal $\boldsymbol{y}(t)$, the manipulated input signal $\boldsymbol{u}(t)$, and the output disturbance $\boldsymbol{d}(t)$ signal, respectively. The input signal $\boldsymbol{u}$ is constrained such that

$$u_i^{\min} \le u_i(t) \le u_i^{\max} \quad i = 1, \ldots, m \tag{2}$$

This can be represented by the saturation function sat(.) defined as

$$\mathrm{sat}(\boldsymbol{u}(\boldsymbol{t})) = \begin{bmatrix} \mathrm{sat}(\boldsymbol{u_1}(\boldsymbol{t})) \\ \vdots \\ \mathrm{sat}(\boldsymbol{u_m}(\boldsymbol{t})) \end{bmatrix} \tag{3}$$

where

$$\mathrm{sat}(u_i(t)) = \begin{cases} u_i^{\max} & u_i > u_i^{\max} \\ u_i & u_i^{\min} \le u_i \le u_i^{\max} \\ u_i^{\min} & u_i < u_i^{\min} \end{cases} \tag{4}$$

denotes the saturation nonlinearity associated with each of the manipulated input $u_i(t)$. The system characteristic matrix $\mathcal{C}$, which describes the transient behavior of the system Eq. (1), is defined for a square system as[11]

$$\mathcal{C} = \lim_{s\to\infty}[\mathrm{diag}\{s^{r_m}\}G] \text{ or } \lim_{z\to\infty}[\mathrm{diag}\{z^{r_m}\}G] \tag{5}$$

where $r_i = \min(r_{i1}, r_{i2}, \ldots, r_{im})$ and $r_{i,j}$ is the relative order of output y_i with respect to manipulated input u_j.

The IMC Antiwindup

The IMC structure evolution

The standard IMC structure introduced in Ref. 25 is illustrated in Figure 1, where G, G_{22}, and Q denote the plant, the model of the plant, and the IMC controller, respectively. The design of Q for optimal performance and robustness is well discussed in the literature.[2,17] With the assumption of perfect model, i.e., $G = G_{22}$, the stability of G and Q guarantees nominal stability of the unsaturated closed-loop system.[17]

However, for saturating system where the actual plant input is $\boldsymbol{v}(\boldsymbol{t}) = \mathrm{sat}(\boldsymbol{u}(\boldsymbol{t}))$, the standard IMC implementation can lead to significant performance degradation, and, therefore nominal stability is no longer guaranteed.[17] In this case,

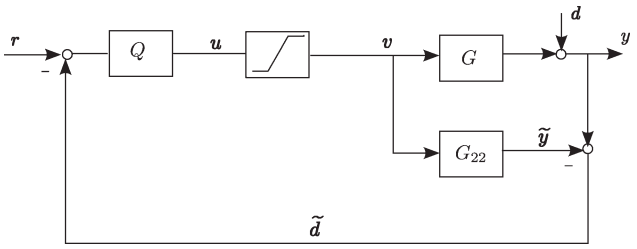

Figure 2. The conventional IMC antiwindup structure.

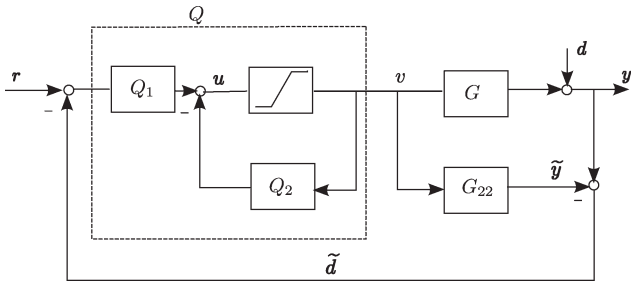

Figure 3. The modified IMC antiwindup structure.

the plant and the model are driven by different inputs. The resultant model/plant mismatch is shown in the following closed-loop equation

$$\boldsymbol{u} = Q(\boldsymbol{r} - \boldsymbol{d}) + QG(\boldsymbol{u} - \boldsymbol{v}) \tag{6}$$

A first step toward avoiding the state mismatch between the plant and the model is the conventional IMC antiwindup structure of Figure 2.[2,17] Although closed-loop nominal stability is guaranteed when there is no model mismatch, the nonlinear performance may be excessively sluggish. The closed-loop equation. Eq (7) shows that the saturation effect on the plant output is not fed back directly to the controller. The controller only acts on the error between the reference signal r and the output disturbance $\boldsymbol{d}$.

$$\boldsymbol{u} = Q(\boldsymbol{r} - \boldsymbol{d}) \tag{7}$$

$$\boldsymbol{y} = G\boldsymbol{v} + \boldsymbol{d} \tag{8}$$

The modified IMC structure shown in Figure 3 was proposed as an antiwindup scheme to deal with the pronounced performance deterioration associated with the standard IMC structure.[2] Assuming no plant model mismatch, the closed loop equations are given by

$$\boldsymbol{u} = Q_1(\boldsymbol{r} - \boldsymbol{d}) - Q_2\boldsymbol{v} \tag{9}$$

$$\boldsymbol{y} = G\boldsymbol{v} + \boldsymbol{d} \tag{10}$$

where $Q = (I + Q_2)^{-1}Q_1$. Here, the controller not only acts on the error between the reference signal and the output disturbance but it is also fed directly with information on the saturating control actions. When the system is away from saturation (i.e., $\boldsymbol{v} = \boldsymbol{u}$), Eq. 9 and 10 reduce to the closed loop equations for the implementation in Figure 1. For a given Q, there are different ways of assigning Q_1 and Q_2. It is imperative that appropriate choices are made to achieve a good nonlinear performance while ensuring stability. One factorization option is[2]

$$Q_1 = \Lambda Q + (I - \Lambda)Q(\infty) \tag{11}$$

where $\Lambda = \lambda I$ is a diagonal weighting matrix and $\lambda \in [0, 1]$. The choice of $\lambda = 1$ results in the conventional IMC structure that chops off the control input resulting in performance deterioration (sluggish response); however, nominal stability is guaranteed. On the other hand, the choice of $\lambda = 0$ corresponds to the factorization proposed in Ref. 20. The performance in this case can be greatly improved; however, nominal stability of the closed-loop system is not guaranteed. Trade off between performance and stability can therefore be achieved by appropriate choice of λ, provided Q is of minimum phase.[2]

Directionality compensators for multivariable IMC

Performance deterioration in multivariable plant with input saturation can be attributed to two major factors. These are the problems resulting from control windup and that of directional change in control. To ensure a graceful performance degradation in the presence of input saturation, a particular choice of Q_1 and possibly an additional nonlinear element in the form of directionality compensator is often incorporated into the controller as shown in Figure 4.[1–3,11,12,21,22,24,27] In this section, a brief review of some of the existing directionality compensator designs is presented within the IMC framework.

The modified IMC antiwindup structure of Figure 3 can be considered as a special case of the scheme in Figure 4, where the directionality compensator NL = I. However, to preserve the output direction,[2] recommend the choice

$$Q_1 = f_A G Q \tag{12}$$

where f_A is a noncausal filter that must be chosen such that $f_A G|_{s=\infty} = I$ or $f_A G|_{z=\infty} = I$ and Q_1 is of minimum phase. These conditions ensure that Q_2 is strictly proper, which guarantees that there is no algebraic loop in the interconnection of Figure 4. It should be noted that the choice $f_A = G^{-1}$ is equivalent to choosing $\lambda = 1$ as in Eq. 11.

In the Direction Preservation (DP) approach,[1] the constrained control action is obtained by scaling down the controller outputs so that the $\boldsymbol{u}$ and $\boldsymbol{v}$ have same direction in the event of saturation. The nonlinearity block NL in Figure 4 is defined as

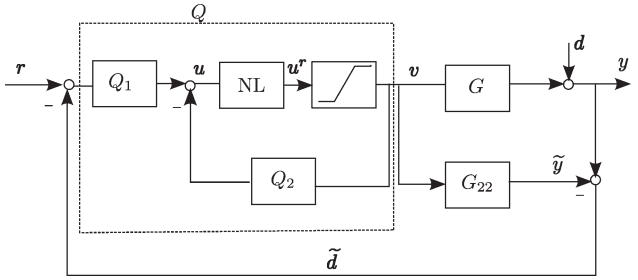

Figure 4. The modified IMC structure with directionality compensation.

Table 1. Performance Comparison of Multivariable Antiwindup Schemes

	Modified IMC	Direction Preservation	Conditioning Technique	Optimal Dynamic Compensation	Optimal Steady State
Transient performance	Optimal	Poor	Optimal	Optimal	Poor
Steady-state performance	Poor	Good	Poor	Poor	Optimal

$$\boldsymbol{u}^r = \mathrm{NL}(\boldsymbol{u}) = \begin{cases} \boldsymbol{u} & \text{if } \boldsymbol{u} \text{ is in linear region} \\ \min\left\{\frac{\mathrm{sat}(u_i)}{u_i}\right\}\boldsymbol{u} & \text{if } \boldsymbol{u} \text{ enters saturation} \end{cases} \quad (13)$$

In this case, subsequent saturation will have no effect because its input $\boldsymbol{u}^r$ always remains in the linear region. The concept of directional preservation has been shown to be beneficial for some class of constrained multivariable control problems.[1,3,12]

A number of optimization based conditioning techniques (OCTs) have also been proposed in the literature.[20–22] All these are extensions of the conditioning techniques originally discussed in Ref. 19, which is based on the concept of realizable reference denoted as $\boldsymbol{w}^r$. When a controller output is infeasible, a realizable control input $\boldsymbol{u}^r$ is obtained by solving an online optimization problem such that the realizable reference $\boldsymbol{w}^r$ is as close as possible to the actual process set point $\boldsymbol{r}$. Following the development in Ref. 21, the NL is defined as

$$\boldsymbol{u}^r = \arg\min_{\boldsymbol{u}^r} \|D_k^{-1}\boldsymbol{u}^r - D_k^{-1}\boldsymbol{u}\|_{\mathcal{W}}^2 \quad (14)$$

subject to the constraints

$$u_i^{\min} \le u_i^r \le u_i^{\max} \quad i = 1, \ldots, m$$

where D_k is the nonsingular feedthrough matrix of the equivalent classical feedback controller K. The relationship between K and Q can be derived as $K = Q(I - G_{22}Q)^{-1}$. We note that for strictly proper system, $D_k = K(\infty) = Q(\infty)$. The positive definite matrix $\mathcal{W}$ takes into account the relative importance of achieving the objectives represented by each component of $\boldsymbol{u}_r$. To address the optimality questions associated with both the modified IMC and DP schemes,[11] The authors in ref 11 have suggested the optimal dynamic compensator (ODC) by solving the following optimization problem

$$\min_{\boldsymbol{u}^r} \|P\mathcal{C}\boldsymbol{u}^r - P\mathcal{C}\boldsymbol{u}\|_{\mathcal{W}}^2 \quad (15)$$

subject to the constraints

$$u_i^{\min} \le u_i^r \le u_i^{\max} \quad i = 1, \ldots, m$$

where P is a diagonal matrix whose diagonal elements depend on the relative orders of each of the controlled output, $\mathcal{C}$ is the characteristic matrix of the plant, and $\mathcal{W}$ is a positive definite weighting matrix. In this approach, the characteristic matrix $\mathcal{C}$ contains information about the directional nature of the plant; thus, the constrained optimization of Eq. 15 is such that the components of $\boldsymbol{u}^r - \boldsymbol{u}$ in the high-gain plant direction are minimized. However, as the characteristic matrix only characterizes the sensitivity of plant to input changes over a very short horizon, the optimality of the solution is only guaranteed over a very short-time horizon.[11] The use of steady-state structural properties such as the steady state gain was suggested in Ref. 24, but only in the context of cross directional control. The scheme in Ref. 24 guarantees optimal steady-state performance by solving the following optimization problem

$$\min_{\boldsymbol{u}^r} \|\mathcal{K}_{\mathrm{p}}\boldsymbol{u}^r - \mathcal{K}_{\mathrm{p}}\boldsymbol{u}\|_{\mathcal{W}}^2 \quad (16)$$

subject to the constraints

$$u_i^{\min} \le u_i^r \le u_i^{\max} \quad i = 1, \ldots, m \quad (17)$$

where $\mathcal{W}$ is a positive definite symmetric matrix, and $\mathcal{K}_{\mathrm{p}}$ is the steady-state gain $G(0)$ [or $G(1)$ for discrete systems]. The steady-state gain can be obtained from the plant's state-space matrices as $G(0) = -CA^{-1}B$ for $G(s)$ [or $G(1) = C(I - A)^{-1}B$ for $G(z)$], provided A (or $I - A$) is nonsingular. This scheme may lead to a degraded transient performance especially when $\mathcal{K}_{\mathrm{p}}$ is significantly different from $\mathcal{C}$.

In Table 1, we categorize these antiwindup schemes according to their performance characteristics during transient stage and steady state when one or more of the input constraints are active. None of the schemes guarantees optimal performance at both phases.

Two-Stage Multivariable IMC Antiwindup Structure

We now consider the two-stage IMC antiwindup scheme of Figure 5. The approach is based on the solution of two quadratic programs (QP) termed the dynamic QP and the steady-state QP. While the former addresses the transient behavior of the plant and ensures that the constrained plant response is as close as possible to the unconstrained plant response, the latter ensures optimal steady-state performance and it is based on steady-state properties of the plant. The idea of using a separate QP to calculate steady-state set points has been previously introduced in MPC formulations.[7–9,28]

Because of the presence of saturation nonlinearities in the system, the output of the constrained system $\boldsymbol{y}$ differs from

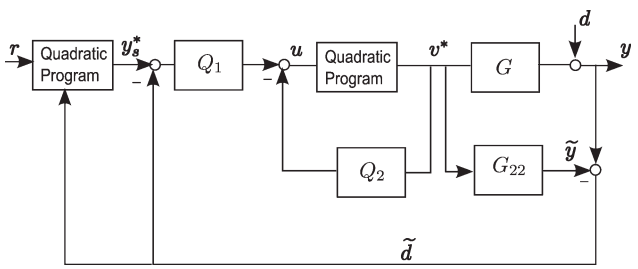

Figure 5. The two-stage IMC antiwindup.

$\boldsymbol{y}'$, the output of the unconstrained system. In general, the control objective is to keep every output $\boldsymbol{y}$ of the constrained system as close as possible to those of the unconstrained system $\boldsymbol{y}'$. We define the mapping

$$\boldsymbol{y}' = \mathcal{P}\boldsymbol{u} \quad \text{and} \quad \boldsymbol{y} = \mathcal{P}\boldsymbol{v} \tag{18}$$

where $\mathcal{P}$ represents the plant operator. $\boldsymbol{v}$ and $\boldsymbol{u}$ are the constrained and unconstrained control inputs, respectively. Mathematically, we seek a feasible control input $\boldsymbol{v}^*$ that is a solution to the following constrained optimization problem.

$$\boldsymbol{v}^* = \arg\min_{\boldsymbol{v}} \|\mathcal{P}\boldsymbol{v} - \mathcal{P}\boldsymbol{u}\|^2_{\mathcal{W}} \tag{19}$$

subject to the constraints

$$u_i^{\min} \le v_i \le u_i^{\max} \quad i = 1, \ldots, m \tag{20}$$

$\mathcal{W}$ is assumed to be positive definite symmetric matrix.

For the system (Eq. 1) where $p = m$, the initial response of the system output to step change in the input vector depends on the characteristics matrix $\mathcal{C}$.[11,29] Therefore, the plant operator $\mathcal{P}$ can be chosen as the characteristic matrix $\mathcal{C}$ of the plant. Making this substitution in Eq. 19 results in the following optimization problem

$$\boldsymbol{v}^* = \arg\min_{\boldsymbol{v}} \|\mathcal{C}\boldsymbol{v} - \mathcal{C}\boldsymbol{u}\|^2_{\mathcal{W}} \tag{21}$$

subject to the constraints

$$u_i^{\min} \le v_i \le u_i^{\max} \quad i = 1, \ldots, m$$

The steady-state aspect of the control problem is to determine appropriate values of ($\boldsymbol{y}_\mathbf{s}$ and $\boldsymbol{u}_\mathbf{s}$) satisfying

$$\boldsymbol{y}_\mathbf{s} = \mathcal{K}_\mathrm{p}\boldsymbol{u}_\mathbf{s} + \tilde{\boldsymbol{d}} \tag{22}$$

where $\boldsymbol{u}_\mathbf{s}$ is the steady-state control input that makes the controlled variable achieve $\boldsymbol{y}_\mathbf{s}$ in steady-state. $\tilde{\boldsymbol{d}}$ is the disturbance estimate obtained as the difference between the measured plant output $\boldsymbol{y}$ and the model output $\tilde{\boldsymbol{y}}$. $\mathcal{K}_\mathrm{p}$ is the nonsingular steady-state gain of the plant. Ideally, $\boldsymbol{y}_\mathbf{s} = \boldsymbol{r}$. If, however, the input constraints are active in steady-state, then $\boldsymbol{y}_\mathbf{s}$ may not attain the target prescribed by the reference signal $\boldsymbol{r}$. The objective is then to find feasible $\boldsymbol{y}_\mathbf{s}$ (or $\boldsymbol{u}_\mathbf{s}$) such that $\boldsymbol{y}_\mathbf{s}$ is as close as possible to $\boldsymbol{r}$ in some sense and within the limit imposed by the input constraints.

The solution of the following QP can be used to determine a feasible steady-state target $\boldsymbol{y}_\mathbf{s}$ that should be applied as shown in Figure 5 such that the closed-loop response in steady state $\boldsymbol{y}_\mathbf{s}$ is as close as possible to $\boldsymbol{r}$.

$$\boldsymbol{y}_\mathbf{s}^* = \arg\min_{\boldsymbol{u}_\mathbf{s}, \boldsymbol{y}_\mathbf{s}} \|\boldsymbol{r} - \boldsymbol{y}_\mathbf{s}\|^2_{\mathcal{Q}_\mathrm{ss}} \tag{23}$$

subject to the constraints

$$u_i^{\min} \le u_{\mathrm{s}_i} \le u_i^{\max} \quad i = 1, \ldots, m \qquad \begin{bmatrix} -\mathcal{K}_\mathrm{p} & I \end{bmatrix} \begin{bmatrix} \boldsymbol{u}_\mathbf{s} \\ \boldsymbol{y}_\mathbf{s} \end{bmatrix} = \tilde{\boldsymbol{d}}$$

where $\mathcal{Q}_\mathrm{ss}$ is a positive definite symmetric matrix for penalizing deviations in each of the controlled variables and their relative importance. The equality constraint guarantees the steady-state requirement of Eq. 22. If the set-point target is achievable in steady state, the difference between the reference signal $\boldsymbol{r}$ and the current disturbance estimate $\tilde{\boldsymbol{d}}$ is passed to the dynamic optimization problem for computation of the control input $\boldsymbol{v}$. If, on the other hand, the steady-state target is not achievable due to the violation of one or more of the constraints in steady state, a feasible steady-state target $\boldsymbol{y}_\mathbf{s}$ is computed such that $\boldsymbol{y}_\mathbf{s}$ is as close as possible to the reference signal $\boldsymbol{r}$. The difference between the feasible steady-state target and the current disturbance estimate is then passed to the dynamic optimization problem.

The equality constraint can be eliminated from Eq. 23 to obtain an equivalent optimization problem

$$\boldsymbol{u}_\mathbf{s}^* = \arg\min_{\boldsymbol{u}_\mathbf{s}} \|\boldsymbol{r} - \tilde{\boldsymbol{d}} - \mathcal{K}_\mathrm{p}\boldsymbol{u}_\mathbf{s}\|^2_{\mathcal{Q}_\mathrm{ss}} \tag{24}$$

subject to the constraints

$$u_i^{\min} \le u_{\mathrm{s}_i} \le u_i^{\max} \quad i = 1, \ldots, m$$

This transformed problem optimizes over variable $\boldsymbol{u}_\mathbf{s}$ and takes as input the difference between the reference signal $\boldsymbol{r}$ and the disturbance estimate $\tilde{\boldsymbol{d}}$. If $\boldsymbol{u}_\mathbf{s}^*$ is an optimal solution of Eq. 24, then the optimal solution $\boldsymbol{y}_\mathbf{s}^*$ of the original problem (Eq. 23) is obtained via the steady-state model of Eq. 22.

The two artificial nonlinearities. Eqs (21 and 24) may be rewritten in the standard QP form as

$$\begin{aligned} \boldsymbol{v}^* &= \arg\min \frac{1}{2}\boldsymbol{v}^T H_1 \boldsymbol{v} - \boldsymbol{v}^T H_1 \boldsymbol{u} \\ &\text{subject to } L\boldsymbol{v} \preceq \boldsymbol{b} \end{aligned} \tag{25}$$

$$\begin{aligned} \boldsymbol{u}_\mathbf{s}^* &= \arg\min \frac{1}{2}\boldsymbol{u}_\mathbf{s}^T H_2 \boldsymbol{u}_\mathbf{s} - \boldsymbol{u}_\mathbf{s}^T \tilde{H}_2^T (\boldsymbol{r} - \tilde{\boldsymbol{d}}) \\ &\text{subject to } L\boldsymbol{u}_\mathbf{s} \preceq \boldsymbol{b} \end{aligned} \tag{26}$$

where $H_1 = \tilde{H}_1^T \tilde{H}_1$ and $H_2 = \tilde{H}_2^T \tilde{H}_2$ are symmetric positive definite Hessian matrices defined in terms of the plant structural properties, i.e., $\tilde{H}_1 = \mathcal{C}$ and $\tilde{H}_2 = \mathcal{K}_\mathrm{p}$. The fixed terms L and $\boldsymbol{b}$ in the inequality constraints are obtained as

$$L = \begin{bmatrix} -I_m \\ I_m \end{bmatrix} \text{ and } \boldsymbol{b} = \begin{bmatrix} -\boldsymbol{u}^{\min} \\ \boldsymbol{u}^{\max} \end{bmatrix} \tag{27}$$

with $\boldsymbol{u}^{\min} = [u_1^{\min}, \cdots, u_m^{\min}]^T$ and $\boldsymbol{u}^{\min} = [u_1^{\max}, \cdots, u_m^{\max}]^T$. The solutions $\boldsymbol{v}^*$ and $\boldsymbol{u}_s^*$ of Eqs. 25 and 26 are unique if the characteristics matrix $\mathcal{C}$ and the steady-state gain $\mathcal{K}_\mathrm{p}$ are nonsingular. We now summarize the first contribution of this article in the following control algorithm.

Two-stage IMC antiwindup control algorithm

Given an open-loop stable plant G with a nominal model G_{22}, and feasible optimal values $\boldsymbol{v}^*$ and $\boldsymbol{u}^*$ satisfying Eqs. 25 and 26, respectively. The control law that achieves combined optimal transient and steady-state performance for the two-stage IMC antiwindup structure of Figure 5 is given by

$$\begin{aligned}\tilde{\boldsymbol{d}} &= \boldsymbol{y} - G_{22}\boldsymbol{v}^* \\ \boldsymbol{u}_s^* &= \psi_2(\boldsymbol{r}, \tilde{\boldsymbol{d}}) \\ \boldsymbol{y}_s^* &= \tilde{H}_2\boldsymbol{u}_s^* + \tilde{\boldsymbol{d}} \\ \boldsymbol{u} &= Q_1(\boldsymbol{y}_s^* - \tilde{\boldsymbol{d}}) - Q_2\boldsymbol{v}^* \\ \boldsymbol{v}^* &= \psi_1(\boldsymbol{u})\end{aligned} \tag{28}$$

where ψ_1 and ψ_2 are nonlinear functions representing the QPs, i.e., Eqs. 25 and 26, respectively.

Without the constraints, the control law reduces to the unconstrained standard IMC control equation

$$\begin{aligned}\tilde{\boldsymbol{d}} &= \boldsymbol{y} - G_{22}\boldsymbol{u} \\ \boldsymbol{u} &= (I + Q_2)^{-1}Q_1(\boldsymbol{r} - \tilde{\boldsymbol{d}})\end{aligned} \tag{29}$$

Correct steady-state behavior is ensured by designing Q such that $Q(0) = G(0)^{-1}$ for $G(s)$ or $Q(1) = G(1)^{-1}$ for $G(z)$. If constraints are active in steady state, then optimal steady-state behavior is guaranteed by solving Eq. 24 subject to the constraints.

Remark 1. For the class of systems whose characteristics matrix $\mathcal{C}$ and steady-state gain $\mathcal{K}_p$ are similar, the optimization problem in Eqs. 21 effectively meets the steady-state requirement of Eq. 24. Hence, only Eq. 21 needs to be solved to achieve both optimal transient and steady-state responses in the presence of control input saturation.

Example 1. *Consider the following example taken from Ref. 2, where*

$$G(s) = \frac{10}{100s+1}\begin{bmatrix} 4 & -5 \\ -3 & 4 \end{bmatrix} \tag{30}$$

with $|u_i| \le 1$, $i = 1,2$ and a step reference input of $[0.63\ 0.79]^T$.

The classical IMC controller design for a step input is

$$Q(s) = \frac{100s+1}{10(20s+1)}\begin{bmatrix} 4 & 5 \\ 3 & 4 \end{bmatrix} \tag{31}$$

and the corresponding unity feedback controller is

$$K(s) = \frac{100s+1}{200s}\begin{bmatrix} 4 & 5 \\ 3 & 4 \end{bmatrix} \tag{32}$$

Following the development in Ref. 2, the plant model is slightly modified as

$$\widetilde{G}(s) = \frac{10}{100s+1}\begin{bmatrix} 4 & \frac{-5}{0.1s+1} \\ \frac{-3}{0.1s+1} & 4 \end{bmatrix} \tag{33}$$

to satisfy the requirement of $f_A G(s)|_{s=\infty} = I$. The noncausal filter f_A is then designed for $\widetilde{G}(s)$ such that $f_A\,\widetilde{G}(s)|_{s=\infty} = I$, where $f_A = 2.5(s+1)I$. The factorization of $Q(s)$ is obtained as $Q_1 = f_A\,\widetilde{G}Q$. In this example,

$$\mathcal{K}_p = \begin{bmatrix} 40 & -50 \\ -30 & 40 \end{bmatrix},\ \mathcal{C} = \begin{bmatrix} 0.4 & -0.5 \\ -0.3 & 0.4 \end{bmatrix},$$

$$\text{and } D_k^{-1} = \begin{bmatrix} 8 & -10 \\ -6 & 8 \end{bmatrix}$$

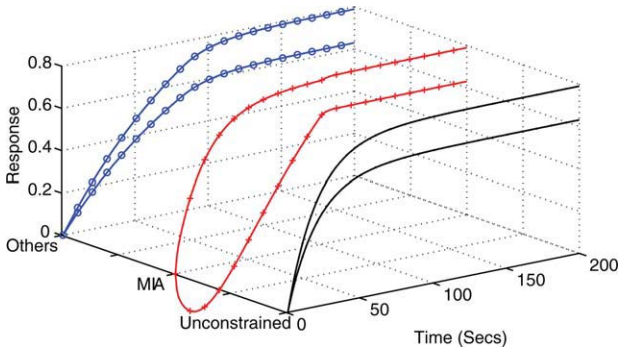

Figure 6. Example 1: The modified IMC antiwindup (MIA, '+') yields a faster response for the first output at the expense of a poor transient response in the second output, whereas the other schemes (DP, OCT, ODC, OSS, and two-stage IMC, 'o') all yield same response.

[Color figure can be viewed in the online issue, which is available at wileyonlinelibrary.com.]

Observe that

$$\mathcal{C} = \frac{1}{100}\mathcal{K}_p \quad \text{and} \quad D_k^{-1} = \frac{1}{5}\mathcal{K}_p$$

so the directionality compensators of Eqs. 14 and 15 are equivalent and effectively meet the criterion for optimal nominal steady-state performance of Eq. 16. This is depicted in Figure 6 where the closed-loop responses for DP,[1] OCT,[21] ODC,[11] and OSS[24] schemes are the same.

Example 2. *This example is taken from Ref. 11 where the state-space model of the process is given as*

$$\begin{bmatrix} \dot{x}_1 \\ \dot{x}_2 \end{bmatrix} = \begin{bmatrix} -0.01 & -0.0002 \\ -0.5 & -0.03 \end{bmatrix}\begin{bmatrix} x_1 \\ x_2 \end{bmatrix} + \begin{bmatrix} 0.25 & 0 \\ 0 & 4 \end{bmatrix}\begin{bmatrix} u_1 \\ u_2 \end{bmatrix}$$

$$\begin{bmatrix} y_1 \\ y_2 \end{bmatrix} = \begin{bmatrix} 1 & 0 \\ 0 & 1 \end{bmatrix}\begin{bmatrix} x_1 \\ x_2 \end{bmatrix} \tag{34}$$

with $|u_1| \le 0.12$ and $|u_2| \le 0.12$ and a set point change of $[0.85\ 2.2]^T$.

The plant can be represented in continuous-time transfer function as

$$G(s) = \begin{bmatrix} \frac{0.25(s+0.003)}{s^2+0.04s+0.0002} & \frac{-0.0008}{s^2+0.04s+0.0002} \\ \frac{-0.125}{s^2+0.04s+0.0002} & \frac{4(s+0.01)}{s^2+0.04s+0.0002} \end{bmatrix} \tag{35}$$

The classical IMC controller design for a step input is

$$Q(s) = \begin{bmatrix} \frac{4s+0.04}{5s+1} & \frac{0.0008}{2s+1} \\ \frac{0.125}{5s+1} & \frac{0.25s+0.0075}{2s+1} \end{bmatrix} \tag{36}$$

and the corresponding unity feedback controller is

$$K(s) = \begin{bmatrix} \frac{4s+0.04}{5s} & \frac{0.0008}{2s} \\ \frac{0.125}{5s} & \frac{0.25s+0.0075}{2s} \end{bmatrix} \tag{37}$$

The controller $Q(s)$ is factorized based on the modified IMC approach as $Q_1 = f_A GQ$ and $Q_2 = f_A G - I$ with

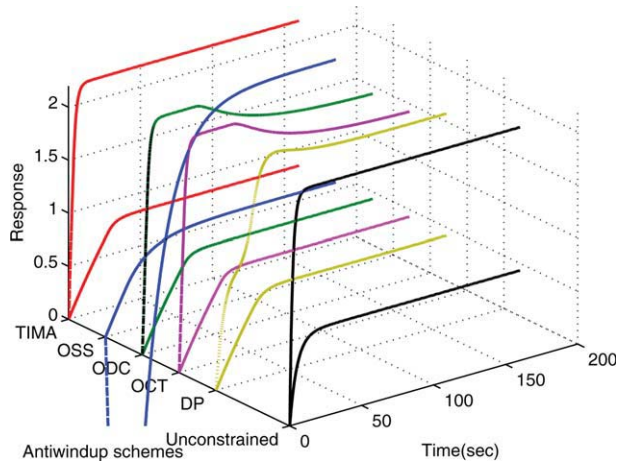

Figure 7. Example 2: Two-stage IMC (TIMA) yields the closest performance to the unconstrained case.

DP and OSS schemes have improved steady-state behaviors but poor transient characteristics as opposed to the OCT and ODC schemes, both of which have optimal transient behaviors but degraded steady-state performances. [Color figure can be viewed in the online issue, which is available at wileyonlinelibrary.com.]

$$f_A = \begin{bmatrix} 4(s+1) & 0 \\ 0 & 0.25(s+1) \end{bmatrix} \tag{38}$$

With relative orders $r_1 = 1$ and $r_2 = 1$, the plant structural matrices are given as

$$\mathcal{K}_p = \begin{bmatrix} 37.5 & -4 \\ -625 & 200 \end{bmatrix}, \quad \mathcal{C} = \begin{bmatrix} 0.25 & 0 \\ 0 & 4 \end{bmatrix},$$

$$D_k^{-1} = \begin{bmatrix} 0.8 & 0 \\ 0 & 0.125 \end{bmatrix}$$

The plant has a diagonal characteristic matrix that is significantly different from the steady-state gain matrix, and, hence, the ODC[11] will result in a different steady-state performance when compared with the OSS[24] scheme. Figure 7 shows the two-stage IMC results in the closest closed-loop

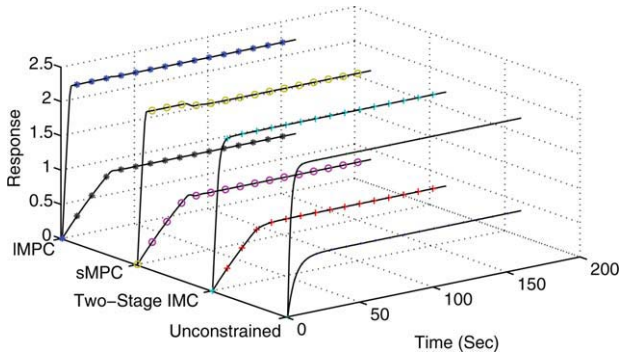

Figure 8. Two-stage IMC ('+') outperforms the single-horizon MPC (sMPC 'o') and yields similar reponse to long-horizon MPC (IMPC '*').

[Color figure can be viewed in the online issue, which is available at wileyonlinelibrary.com.]

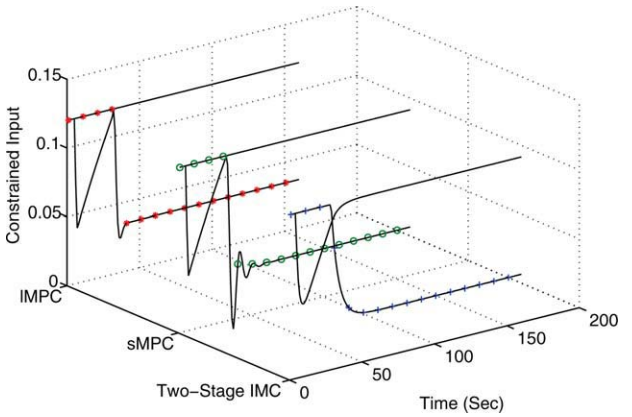

Figure 9. Constrained input: two-stage IMC ('+'), single-horizon MPC (sMPC 'o'), and long-horizon MPC (IMPC '*').

[Color figure can be viewed in the online issue, which is available at wileyonlinelibrary.com.]

performance to the unconstrained case when compared with the other antiwindup schemes.

We also compare the performance of the two-stage IMC with a particular MPC formulation.[10] We consider two MPC cases; a single-horizon MPC (prediction horizon $N_p = 1$ and control horizon $N_c = 1$) and a long-horizon MPC (prediction horizon $N_p = 100$ and control horizon $N_c = 50$). The closed-loop responses in Figures 8 and 9 show that the two-stage IMC competes favorably with a long-horizon MPC while only requiring the computation equivalent to that of a single-horizon MPC.[30] However, it is envisaged that a long-horizon MPC will outperform the two-stage IMC especially when there are high-order unmodeled dynamics in the system. The two-stage IMC does not require the receding horizon computation of MPC and may serve as a less computationally intensive and more transparent (in terms of tuning for robustness) alternative to MPC.

Stability Analysis

We assume the plant as represented in Figure 10, where G maps $\boldsymbol{q}_\Delta,\boldsymbol{v}$ to $\boldsymbol{p}_\Delta,\boldsymbol{y}$ according to

$$\begin{bmatrix} \boldsymbol{p}_\Delta \\ \boldsymbol{y} \end{bmatrix} = \begin{bmatrix} G_{11} & G_{12} \\ G_{21} & G_{22} \end{bmatrix} \begin{bmatrix} \boldsymbol{q}_\Delta \\ \boldsymbol{v} \end{bmatrix} \tag{39}$$
$$\boldsymbol{q}_\Delta = \Delta \boldsymbol{p}_\Delta$$

and Δ is a causal, linear time invariant (LTI) operator satisfying $\|\Delta\|_\infty < 1$.

The transfer function from $\boldsymbol{v}$ to $\boldsymbol{y}$ is given by

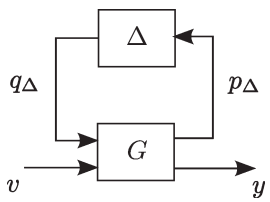

Figure 10. General plant uncertainty description.

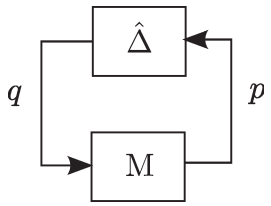

Figure 11. General feedback interconnection for stability analysis.

$$\boldsymbol{y} = [G_{22} + G_{21}\Delta(I - G_{11}\Delta)^{-1}G_{12}]\boldsymbol{v} \tag{40}$$

where G_{22} is the nominal model, and G_{11}, G_{12}, and G_{21} are known transfer functions. A number of unstructured uncertainty descriptions can be put into this general form.[31] For example, feedback uncertainty description is obtained by setting

$$G = \begin{bmatrix} -W_1G_{22}W_2 & W_1G_{22} \\ -G_{22}W_2 & G_{22} \end{bmatrix} \tag{41}$$

Similarly, additive or multiplicative uncertainty descriptions can be obtained by setting

$$G = \begin{bmatrix} 0 & W_1 \\ W_2 & G_{22} \end{bmatrix} \text{ or } G = \begin{bmatrix} 0 & W_1G_{22} \\ W_2 & G_{22} \end{bmatrix} \tag{42}$$

where W_1 and W_2 are frequency-dependent stable transfer functions.

Following the convention of optimizing antiwindup designs, artificial nonlinearities are introduced such that the input saturation nonlinearities are never active and may be safely ignored as shown in Figure 5.

For the purpose of stability analysis, we consider the standard feedback interconnection of Figure 11, where all exogenous inputs and output signals have been ignored. M is a LTI system operator, and $\hat{\Delta}$ is a block diagonal operator defined by

$$\hat{\Delta} = \{\text{diag}(\psi_1, \ldots, \psi_m, \Delta_1, \ldots, \Delta_k)\} \tag{43}$$

where ψ_i: $l^m[0, \infty) \to l^m[0, \infty)$ is a static operator and Δ_i: $l^{n_i}[0, \infty) \to l^{n_i}[0, \infty)$ is some unknown operator. The input-output map is defined by the equations

$$\boldsymbol{q} = \hat{\Delta}\boldsymbol{p}, \quad \boldsymbol{p} = M\boldsymbol{q} \tag{44}$$

As practical implementations of most control systems require the use of digital devices or computers, we restrict our following discussions to discrete-time systems although continuous-time analysis follows naturally.

Definitions and existing results

Definition 1 (Strongly positive realness (SPR)[32]) SPR.
A square transfer function matrix G is, SPR if

1. G is asymptotically stable.
2. $G(e^{jw}) + G^*(e^{jw})$ is positive definite $\forall w \in [0,2\ \pi]$
3. $G(\infty) + G(\infty)^T > 0$.

Definition 2 (Sector-bound nonlinearity[32]. Let $\psi(\boldsymbol{x},k)$: $\mathbb{R}^m \times \mathbb{N} \to \mathbb{R}^m$ be a memoryless (possibly time varying) nonlinearity and $K = K_1 - K_2 = K^T$ for some $K_1, K_2 \in \mathbb{R}^{m\times m}$. We say $\psi(\boldsymbol{x},k) \in [K_1,K_2]$ if

$$[\phi(\boldsymbol{x},k) - K_1\boldsymbol{x}]^T[\phi(\boldsymbol{x},k) - K_2\boldsymbol{x}] \le 0 \quad \forall\, \boldsymbol{x} \in \mathbb{R}^m \text{ and } k \in \mathbb{N} \tag{45}$$

Certain QPs that must be solved by most optimizing antiwindups and MPC have been shown to satisfy some sector-bound conditions.[27] The following lemmas allow the extension of the sector-bound and the multivariable circle criterion results to such systems.

Lemma 1 (QP as a sector bounded non-linearity[27]).
Let ψ be given by the following general QP

$$\psi(\boldsymbol{x}) = \arg\min_{v} \frac{1}{2}\boldsymbol{v}^T H\boldsymbol{v} - \boldsymbol{v}^T F\boldsymbol{x} \quad \text{subject to} \quad A\boldsymbol{v} \le \boldsymbol{b} \quad \text{with} \quad \boldsymbol{b}\ge 0 \quad \text{and} \quad C\boldsymbol{v} = 0 \tag{46}$$

if H has full rank and $\mathbf{0}$ is always feasible then the static nonlinearity ψ satisfies

$$\psi(\boldsymbol{x})^T H\psi(\boldsymbol{x}) - \psi(\boldsymbol{x})^T F\boldsymbol{x} \le 0\ \forall\ \boldsymbol{x} \tag{47}$$

Proof. See Ref. 27. ■

The QPs (Eqs. 25 and 26) appear as special cases of Eq. 46 and satisfy the generalized sector-bound condition (Eq. 47) with the fixed term F set as H_1 and H_2^T, respectively.

Lemma 2 (Multivariable circle criterion[27,32]) Suppose $\psi(.)$ is given as Eq. 46 and satisfies the sector condition (Eq. 47). If $H + FG(.)$ is SPR, then the feedback interconnection of $\psi(.)$ and the plant $G(.)$ is asymptotically stable.

Proof. See Ref. 27. ■

Definition 3 (IQC[33,34]). Consider the feedback interconnection of Figure 11 and let Π be a bounded and self-adjoint operator. Then Δ satisfies the IQC defined by Π or simply $\Delta \in \text{IQC}(\Pi)$ if.

$$\left\langle \begin{bmatrix} \boldsymbol{p} \\ \boldsymbol{q} \end{bmatrix}, \Pi \begin{bmatrix} \boldsymbol{p} \\ \boldsymbol{q} \end{bmatrix} \right\rangle \ge 0 \tag{48}$$

where $\langle .,. \rangle$ denotes the inner product and Π is an operator satisfying

$$\Pi(e^{jw}) = \Pi^*(e^{jw})\ \forall\ w\ \in [-\pi, \pi] \text{ and } \boldsymbol{p}, \boldsymbol{q} \in l_2[0, \infty) \tag{49}$$

The argument (e^{jw}) will be omitted afterward to maintain compactness of expressions.

If Δ has the block diagonal structure $\Delta = \text{diag}[\Delta_1, \Delta_2]$ and Δ_i satisfies the IQC defined by

$$\Pi_i = \begin{bmatrix} \Pi_{i(11)} & \Pi_{i(12)} \\ \Pi^*_{i(12)} & \Pi_{i(22)} \end{bmatrix} \text{ for } i = 1, 2$$

then, the diagonal operator Δ operator satisfies the IQC defined by

$$\Pi = \text{daug}(\Pi_1, \Pi_2) = \left[\begin{array}{cc|cc} \Pi_{1(11)} & & \Pi_{1(12)} & \\ & \Pi_{2(11)} & & \Pi_{2(12)} \\ \hline \Pi^*_{1(12)} & & \Pi_{2(22)} & \\ & \Pi^*_{2(12)} & & \Pi_{2(22)} \end{array}\right]$$

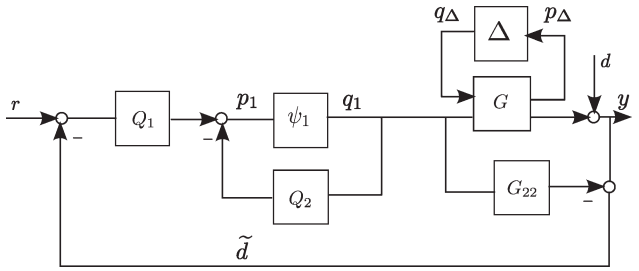

Figure 12. Standard IMC antiwindup with QP for stability analysis.

Here, daug(.) represents the diagonal augmentation of the operators Π_i, $i = 1,2$.

Robust stability analysis of standard IMC antiwindup with a QP

It has been reported in Ref. 35 that robust stability of optimizing antiwindup schemes can be demonstrated using the sector bound condition. Such optimizing antiwindup schemes[2,11,20,22,24] may be realized in the IMC framework of Figure 12, where directionality compensation is introduced via the QP ψ_1 defined in Eq. 25. We have the controller equation as

$$\begin{aligned} \tilde{\boldsymbol{d}} &= \boldsymbol{y} - G_{22}\boldsymbol{q}_1 \\ \boldsymbol{p}_1 &= Q_1(\boldsymbol{r} - \tilde{\boldsymbol{d}}) - Q_2\boldsymbol{q}_1 \\ \boldsymbol{q}_1 &= \psi_1(\boldsymbol{p}_1) \end{aligned} \tag{50}$$

In what follows, we derive the sufficient stability condition using the theory of IQCs.[33,34] The antiwindup structure of Figure 12 can be transformed into the general feedback interconnection of Figure 13 by defining

$$\boldsymbol{p} = \begin{bmatrix} \boldsymbol{p}_\Delta \\ \boldsymbol{p}_1 \end{bmatrix} \quad \text{and} \quad \boldsymbol{q} = \begin{bmatrix} \boldsymbol{q}_\Delta \\ \boldsymbol{q}_1 \end{bmatrix} \tag{51}$$

so that

$$\hat{\Delta} = \begin{bmatrix} \Delta & \\ & \psi_1 \end{bmatrix} \tag{52}$$

$$M = \begin{bmatrix} G_{11} & G_{12} \\ -Q_1G_{21} & -Q_2 \end{bmatrix} \tag{53}$$

We have $\Delta \in \text{IQC}(\Pi_\Delta)$ and $\psi_1 \in \text{IQC}(\Pi_{\psi_1})$ with

$$\Pi_\Delta = \begin{bmatrix} I & \\ & -I \end{bmatrix} \quad \Pi_{\psi_1} = \begin{bmatrix} 0 & H_1 \\ H_1 & -2H_1 \end{bmatrix} \tag{54}$$

It follows immediately that $\Delta \in \text{IQC}(\alpha\Pi_\Delta)$ and $\psi_1 \in \text{IQC}(\beta_1\Pi_{\psi_1})$ for $\alpha, \beta_1 > 0$.

The stability condition for the antiwindup structure of Figure 12 based on the results in Refs. 33 and 34 is stated in the following theorem.

Theorem 1 (IQC stability theorem)

Given a stable plant G (Eq. 39) in feedback interconnection with controller (Eq 50). Let M be the LTI portion of the closed-loop system and Δ and ψ_1 satisfy the IQC defined by Eqs. 48 and 54, respectively, such that we can write

$$\Pi_{\hat{\Delta}} = \left[\begin{array}{cc|cc} \alpha I & & 0 & \\ & 0 & & \beta_1 H_1 \\ \hline 0 & & -\alpha I & \\ & \beta_1 H_1 & & -2\beta_1 H_1 \end{array}\right] \tag{55}$$

Then the closed-loop system is stable provided

$$\begin{bmatrix} M \\ I \end{bmatrix}^* \Pi_{\hat{\Delta}} \begin{bmatrix} M \\ I \end{bmatrix} \leq -\varepsilon I \tag{56}$$

for some $\varepsilon > 0$, for all $w \in [-\pi, \pi]$.

Proof. See Ref. 33.

The condition (Eq. 56) is equivalent to

$$\left[\begin{array}{c|c} S_{11} & S_{12} \\ \hline S_{21} & S_{22} \end{array}\right] \geq \varepsilon I \tag{57}$$

with

$$\begin{aligned} S_{11} &= \alpha(I - G_{11}^* G_{11}) \\ S_{21} &= S_{12}^* = \beta_1 H_1 Q_1 G_{21} - \alpha G_{12}^* G_{11} \\ S_{22} &= \beta_1(H_1 Q_2 + Q_2^* H_1 + 2H_1) - \alpha G_{12}^* G_{12} \end{aligned}$$

For the case where the control input signal is unconstrained such that $Q = (I + Q_2)^{-1}Q_1$ and the plant is given by Eq. 39, stability condition for such systems is well established[17] and may be obtained via the small gain theorem as

$$\|G_{11} - G_{12}QG_{21}\|_\infty \leq 1 \tag{58}$$

For the constrained nominal (perfect model assumption) case, the IMC antiwindup of Figure 12 can be put into the feedback structure of Figure 11 with

$$\hat{\Delta} = \psi_1 \quad \text{and} \quad M = -Q_2 \tag{59}$$

The closed loop consisting of the feedback interconnection defined by Eq. 59 with ψ_1 satisfying Eq. 47 is stable if $(H_1Q_2 + H_1)$ is SPR. We may write this as

$$H_1Q_2 + Q_2^*H_1 + 2H_1 > 0 \tag{60}$$

The stability condition (Eq. 60) follows from direct application of multivariable circle criterion and Lemmas 1 and 2. (See Refs. 27 and 32).

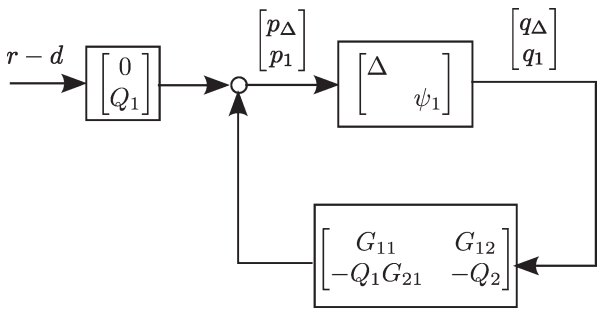

Figure 13. Feedback interconnection for standard IMC antiwindup with QP.

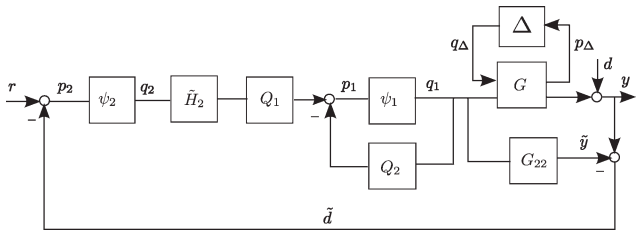

Figure 14. Two-stage IMC antiwindup for stability analysis.

Remark 2. The stability conditions (Eqs. 58 and 60) may also be obtained via the IQC theorem by noting that ψ_1 and Δ satisfy the IQCs defined by Eq. 54. The IQC stability condition (Eq. 56) then reduces to Eqs. 58 and 60.

Robust analysis of two-stage IMC antiwindup

In this section, we consider the robust stability analysis of the two-stage IMC antiwindup scheme. Reorganizing the two-stage structure of Figure 5 in terms of the transformed steady-state QP (Eq. 26), we obtain an equivalent structure of Figure 14. The IMC controller Q is designed *a priori* to meet some nominal performance specifications, and then further augmentations are introduced to deal with performance deterioration in the face of control input saturations and model uncertainties. We analyzed the stability of the two-stage IMC antiwindup for three cases: (a) the robust stability of the unconstrained structure; (b) the constrained nominal stability; and (c) the complete stability involving the input nonlinearities and the model uncertainties.

Unconstrained robust stability analysis For the unconstrained case where $Q = (I + Q_2)^{-1}Q_1$, the two-stage IMC antiwindup scheme reduces to the standard IMC without an antiwindup compensation. In this case, the controller (Eq. 28) reduces to

$$\begin{aligned} \tilde{\boldsymbol{d}} &= \boldsymbol{y} - G_{22}\boldsymbol{q}_1 \\ \boldsymbol{q}_1 &= (I + Q_2)^{-1}Q_1(\boldsymbol{r} - \tilde{\boldsymbol{d}}) = Q(\boldsymbol{r} - \tilde{\boldsymbol{d}}) \end{aligned} \tag{61}$$

The closed-loop is completely described by

$$\begin{aligned} \boldsymbol{q}_\Delta &= \Delta \boldsymbol{p}_\Delta \\ \boldsymbol{p}_\Delta &= (G_{11} - G_{12}QG_{21})\boldsymbol{q}_\Delta + G_{12}Q(\boldsymbol{r} - \boldsymbol{d}) \end{aligned} \tag{62}$$

Robust stability result for this case is standard and can be obtained via the application of small-gain theorem[17] or the IQC theorem.[36]

Result 1. Given a stable plant G (Eq. 39) in feedback interconnection with controller (Eq. 61). Then the closed-loop system is stable for all $\|\Delta\|_\infty < 1$, provided

$$\|G_{11} - G_{12}QG_{21}\|_\infty \le 1 \tag{63}$$

Proof. From the closed-loop equation (Eq. 62), we have $M = G_{11} - G_{12}QG_{21}$ and $\hat{\Delta} = \Delta$. The result follows from the application of IQC stability condition (Eq. 56). ■

Constrained nominal stability analysis

When the plant is assumed to be perfectly known ($G = G_{22}$), the two-stage IMC antiwindup structure becomes a quasi-open loop system as the outer loop in Figure 14 represents a feedforward of the influence of disturbance $\boldsymbol{d}$ and is not affected by the action of the manipulated variable. The only remaining closed-loop is the feedback around the nonlinearity ψ_1. The overall system is stable if and only if both the plant and the algebraic loop are stable. The closed-loop equations around the nonlinearity is given by

$$\begin{aligned} \boldsymbol{q}_1 &= \psi_1(\boldsymbol{p}_1) \\ \boldsymbol{p}_1 &= -Q_2\boldsymbol{q}_1 + Q_1\tilde{H}_2\boldsymbol{q}_2 \\ \boldsymbol{q}_2 &= \psi_2(\boldsymbol{r} - \boldsymbol{d}) \end{aligned} \tag{64}$$

Result 2. Given a stable plant $G = G_{22}$ in feedback interconnection with controller of the form (Eq. 28) with ψ_1 and ψ_2 satisfying the sector-bound condition (Eq. 47). Then the closed-loop antiwindup system is stable provided

$$\beta_1(H_1Q_2 + Q_2^*H_1 + 2H_1) - \frac{\beta_1^2}{2\beta_2}H_1Q_1Q_1^*H_1 \ge \varepsilon I \tag{65}$$

for some ε, β_1, $\beta_2 > 0$, for all $w \in [-\pi, \pi]$

Proof. From Eq. 64, we have

$$M = \begin{bmatrix} -Q_2 & Q_1\tilde{H}_2 \\ 0 & 0 \end{bmatrix} \text{ and } \hat{\Delta} = \begin{bmatrix} \psi_1 & \\ & \psi_2 \end{bmatrix}$$

with ψ_1 and ψ_2 satisfying the IQCs defined by Eqs. 54 and 66, respectively.

$$\Pi_{\psi_2} = \begin{bmatrix} 0 & \tilde{H}_2 \\ \tilde{H}_2^T & -2H_2 \end{bmatrix} \tag{66}$$

$\Pi_{\hat{\Delta}}$ then becomes

$$\Pi_{\hat{\Delta}} = \left[\begin{array}{cc|cc} 0 & & \beta_1 H_1 & \\ & 0 & & \beta_2\tilde{H}_2 \\ \hline \beta_1 H_1 & & -2\beta_1 H_1 & \\ & \beta_2\tilde{H}_2^T & & -2\beta_2 H_2 \end{array}\right] \tag{67}$$

The result follows from the application of IQC stability condition (Eq. 56) followed by the application of Schur complements. ■

Complete stability analysis of two-stage IMC antiwindup

The antiwindup structure of Figure 14 is transformed into the general feedback structure of Figure 15 by defining

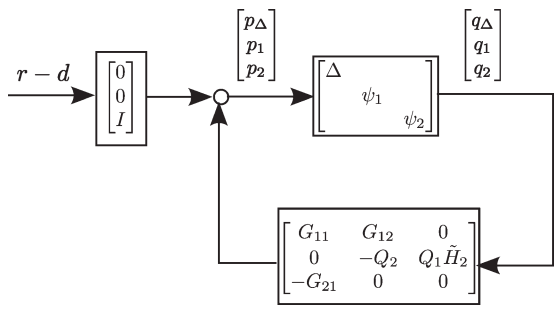

Figure 15. Feedback interconnection for two-stage IMC antiwindup.

$$p = \begin{bmatrix} p_\Delta \\ p_1 \\ p_2 \end{bmatrix} \quad \text{and} \quad q = \begin{bmatrix} q_\Delta \\ q_1 \\ q_2 \end{bmatrix} \tag{68}$$

so that

$$\hat{\Delta} = \begin{bmatrix} \Delta & & \\ & \psi_1 & \\ & & \psi_2 \end{bmatrix} \tag{69}$$

$$M = \begin{bmatrix} G_{11} & G_{12} & 0 \\ 0 & -Q_2 & Q_1\tilde{H}_2 \\ -G_{21} & 0 & 0 \end{bmatrix}. \tag{70}$$

We have $\Delta \in \mathrm{IQC}(\Pi_\Delta)$, $\psi_1 \in \mathrm{IQC}(\Pi_{\psi_1})$ and $\psi_2 \in \mathrm{IQC}(\Pi_{\psi_2})$ where Π_Δ, Π_{ψ_1} and Π_{ψ_2} are as defined in Eqs. 54 and 66.

The $\hat{\Delta}$ defined in Eq. 69 satisfies the IQC $\hat{\Delta} \in \mathrm{IQC}(\Pi_{\hat{\Delta}})$ with

$$\Pi_{\hat{\Delta}} = \begin{bmatrix} \Pi_{11}^{\hat{\Delta}} & \Pi_{12}^{\hat{\Delta}} \\ \Pi_{21}^{\hat{\Delta}} & \Pi_{22}^{\hat{\Delta}} \end{bmatrix} = \mathrm{daug}(\alpha\Pi_\Delta, \beta_1\Pi_{\psi_1}, \beta_2\Pi_{\psi_2}) \tag{71}$$

where

$$\Pi_{11}^{\hat{\Delta}} = \begin{bmatrix} \alpha I & & \\ & 0 & \\ & & 0 \end{bmatrix}, \quad \Pi_{12}^{\hat{\Delta}} = \begin{bmatrix} 0 & & \\ & \beta_1 H_1 & \\ & & \beta_2\tilde{H}_2 \end{bmatrix}$$

$$\Pi_{21}^{\hat{\Delta}} = \begin{bmatrix} 0 & & \\ & \beta_1 H_1 & \\ & & \beta_2\tilde{H}_2^T \end{bmatrix} \quad \text{and}$$

$$\Pi_{22}^{\hat{\Delta}} = \begin{bmatrix} -\alpha I & & \\ & -2\beta_1 H_1 & \\ & & -2\beta_2 H_2 \end{bmatrix}$$

for any choice of multipliers α, β_1, $\beta_2 > 0$. We note that the top left quadrant of $\Pi_{\hat{\Delta}}$ is positive semidefinite ($\Pi_{11}^{\hat{\Delta}} \geq 0$), whereas the bottom right quadrant of $\Pi_{\hat{\Delta}}$ is negative semidefinite ($\Pi_{22}^{\hat{\Delta}} \leq 0$) and so $\tau\hat{\Delta} \in \mathrm{IQC}(\Pi_{\hat{\Delta}})$ for all $0 \leq \tau \leq 1$.

We now state the stability result for the complete two-stage IMC antiwindup structure.

Result 3. Given a stable plant G (Eq. 39) in feedback interconnection with controller of the form (Eq. 28) with Δ, ψ_1 and ψ_2 satisfying the IQC defined by Eqs. 48, 54 and 66, respectively. Then the closed-loop antiwindup system of Figure 14 is stable, provided

$$\left[\begin{array}{c|c} X_{11} & X_{12} \\ \hline X_{21} & X_{22} \end{array}\right] \geq \varepsilon I \tag{72}$$

for some $\varepsilon > 0$, for all $w \in [-\pi, \pi]$ with

$$X_{11} = \alpha(I - G_{11}^* G_{11}) - \frac{\beta_2}{2} G_{21}^* G_{21}$$

$$X_{21} = X_{12}^* = \frac{\beta_1}{2} H_1 Q_1 G_{21} - \alpha G_{12}^* G_{11}$$

$$X_{22} = \beta_1(H_1 Q_2 + Q_2^* + 2H_1) - \alpha G_{12}^* G_{12} - \frac{\beta_1^2}{2\beta_2} H_1 Q_1 Q_1^* H_1$$

Proof. The two-stage IMC antiwindup structure of Figure 14 can be transformed into the general feedback interconnection of Figure 11, with M and $\hat{\Delta}$ defined in Eqs. 70 and 69, respectively. The IQC stability condition of Eq. 56 reduces to

$$\left[\begin{array}{cc|c} \alpha(I - G_{11}^* G_{11}) & -\alpha G_{11}^* G_{12} & \beta_2 G_{21}^* \tilde{H}_2 \\ -\alpha G_{12}^* G_{11} & \beta_1(H_1 Q_2 + Q_2^* H_1 + 2H_1) - \alpha G_{12}^* G_{12} & -\beta_1 H_1 Q_1 \tilde{H}_2 \\ \hline \beta_2 \tilde{H}_2^T G_{21} & -\beta_1 \tilde{H}_2^T Q_1^* H_1 & 2\beta_2 H_2 \end{array}\right] \geq \varepsilon I \tag{73}$$

The result follows after the application of Schur complements to Eq. 73 and using the fact that the bottom right block is positive definite and thus its inverse exists. ■

Note that S and X on the left-hand sides of Eqs. 57 and 72, respectively, are both partitioned Hermitian matrices. Their structures can be exploited to establish a relationship between the robustness of the two-stage IMC antiwindup and the standard IMC antiwindup with a QP.

Remark 3. The condition given in Eq. 57 is a necessary but not sufficient for Eq. 72 to hold. The condition given in Eq. 72 can be expressed as $X = S - Z > 0$, where Z is given as

$$\begin{bmatrix} \frac{\beta_2}{2} G_{21}^* G_{21} & \frac{\beta_1}{2} G_{21}^* Q_1^* H_1 \\ \frac{\beta_1}{2} H_1 Q_1 G_{21} & \frac{\beta_1^2}{2\beta_2} H_1 Q_1 Q_1^* H_1 \end{bmatrix} = \frac{1}{2\beta_2} \begin{bmatrix} \beta_2 G_{21}^* \\ \beta_1 H_1 Q_1 \end{bmatrix} [\, \beta_2 G_{21} \quad \beta_1 Q_1^* H_1 \,] \geq 0 \tag{74}$$

The positive definiteness of X implies that S is also positive definite. On the other hand, X is positive definite if and only if $S > 0$ and $S > Z$.

If M is assumed to have the following minimal state-space representation

$$\begin{bmatrix} A_M & B_M \\ C_M & D_M \end{bmatrix} \sim M = C_M(zI - A_M)^{-1} B_M + D_M \tag{75}$$

where A_M is Hurwitz and the pair (A_M, B_M) is controllable, then the frequency-domain stability condition (Eq. 72) can be transformed into the following linear matrix inequalities via the discrete-time Kalman-Yakubovich-Popov lemma. Then, the system is stable provided that there exists a matrix $P = P^T$ satisfying

$$\begin{bmatrix} A_M^T P A_M - P & A_M^T P B_M \\ B_M^T P A_M & B_M^T P B_M \end{bmatrix} + \Pi \leq 0 \tag{76}$$

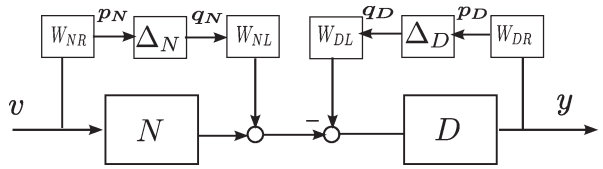

Figure 16. Plant with matrix fraction uncertainty for simulation.

We note that $\Pi_{\hat{\Delta}}$ is static and depends on the positive definite parameters α, β_1, and β_2. Then we may write Π as

$$\Pi = \begin{bmatrix} \Pi_{11} & \Pi_{12} \\ \Pi_{21} & \Pi_{22} \end{bmatrix} \tag{77}$$

with

$$\begin{aligned} \Pi_{11} &= C_M^T \Pi_{11}^{\hat{\Delta}} C_M \\ \Pi_{12} &= \Pi_{21}^* = C_M^T \Pi_{12}^{\hat{\Delta}} + C_M^T \Pi_{11}^{\hat{\Delta}} D_M \\ \Pi_{22} &= \Pi_{22}^{\hat{\Delta}} + \Pi_{21}^{\hat{\Delta}} D_M + D_M^T \Pi_{12}^{\hat{\Delta}} + D_M^T \Pi_{11}^{\hat{\Delta}} D_M \end{aligned} \tag{78}$$

Simulation Example

We now illustrate the stability test for the two-stage IMC antiwindup where the plant nominal model has the following left matrix fraction factorization $D^{-1}N$ such that the perturbed plant (Figure 16) can be expressed as

$$G = (D + W_{\mathrm{DL}} \Delta_{\mathrm{D}} W_{\mathrm{DR}})^{-1} (N + W_{\mathrm{NL}} \Delta_{\mathrm{N}} W_{\mathrm{NR}}) \tag{79}$$

This can be put in the form of Figure 10 with

$$G = \left[\begin{array}{cc|c} 0 & 0 & W_{\mathrm{NR}} \\ W_{\mathrm{DR}} D^{-1} W_{\mathrm{NL}} & -W_{\mathrm{DR}} D^{-1} W_{\mathrm{DL}} & W_{\mathrm{DR}} D^{-1} N \\ \hline D^{-1} W_{\mathrm{NL}} & -D^{-1} W_{\mathrm{DL}} & D^{-1} N \end{array}\right] \tag{80}$$

and

$$\Delta_u = \begin{bmatrix} \Delta_N & \\ & \Delta_D \end{bmatrix}, \quad p_1 = \begin{bmatrix} p_N \\ p_D \end{bmatrix}, \quad q_1 = \begin{bmatrix} q_N \\ q_D \end{bmatrix} \tag{81}$$

where W_{DL}, W_{DR}, W_{NL}, and W_{NR} are weighting transfer function matrices. We will assume that the uncertainties satisfy $\|\Delta_N\|_\infty < 1$ and $\|\Delta_D\|_\infty < 1$ so that $\Delta_u \in \mathrm{IQC}(\Pi_u(\alpha_N, \alpha_D))$ with

$$\Pi_u(\alpha_N, \alpha_D) = \mathrm{diag}(\alpha_N I, \alpha_D I, -\alpha_N I, -\alpha_D I) \tag{82}$$

for any α_N, $\alpha_D > 0$.

Example 3. We consider Example 2 again. The plant is discretized using a sampling time of $T_s = 0.2$ resulting in the following discrete time transfer function matrix description of the nominal plant.

$$G = \frac{1}{\eta} \begin{bmatrix} (4.995z - 4.965)10^{-2} & -(1.596z + 1.591)10^{-5} \\ -(2.493z - 24.87)10^{-2} & (7.976z - 7.96)10^{-1} \end{bmatrix}$$

with $\eta = z^2 - 1.992z + 0.992$ and sampling time. The standard IMC controller designed based on the approach of Ref. 2 for a step input is

$$Q_1 = \begin{bmatrix} 0.8 & 0 \\ 0 & 0.125 \end{bmatrix}$$

$$Q_2 = \frac{1}{\eta} \begin{bmatrix} (3.796z - 3.773)10^{-2} & (-6.537z + 5.914)10^{-3} \\ (-6.502z + 6.247)10^{-4} & (9.372z - 9.353)10^{-2} \end{bmatrix}$$

For the two-stage design, we chose $\tilde{H}_1$ and $\tilde{H}_2$ as the plant characteristic matrix (in the notion of Ref. 11) and the steady-state gain,[37] respectively.

$$\tilde{H}_1 = \begin{bmatrix} 0.25 & 0 \\ 0 & 4 \end{bmatrix} \text{ and } \tilde{H}_2 = \begin{bmatrix} 37.5 & -4 \\ -625 & 200 \end{bmatrix}$$

A time-domain simulation of the plant was carried out for a particular value of model mismatch $\Delta_N = \Delta_D = (0.1z - 0.09602)(z - 0.9881)^{-1}$ with infinity norm of 0.33. The left fraction matrix nominal model for the plant was chosen as $G_{22} = D^{-1}N$ with $N = G_{22}$ and $D = I$. The uncertainty weights

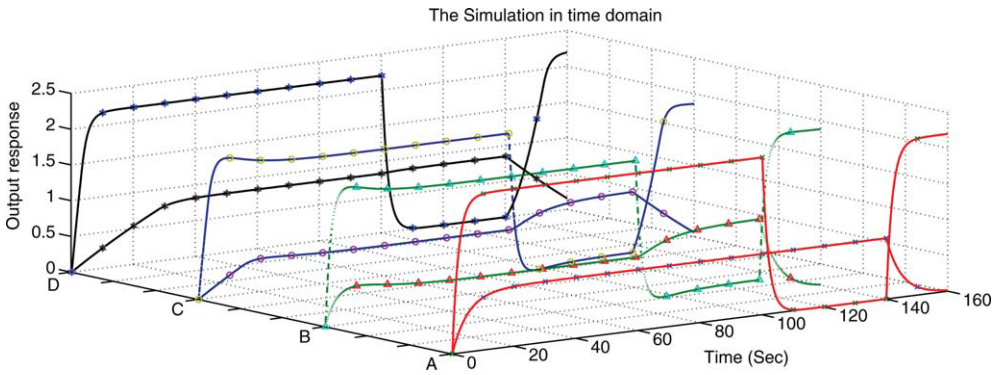

Figure 17. Simulations in time domain.

A: Unconstrained nominal system; B: perturbed unconstrained; C: perturbed with a single-stage IMC AW; D: perturbed with two-stage IMC AW. [Color figure can be viewed in the online issue, which is available at wileyonlinelibrary.com.]

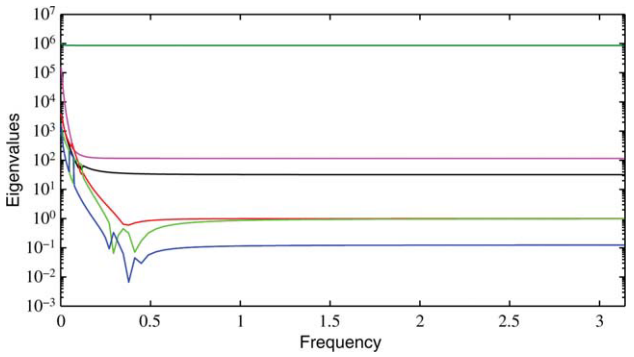

Figure 18. Eigenvalues of X evaluated for all $w \in [0,\pi]$ and with $\alpha = \beta_1 = \beta_2 = 1$.

[Color figure can be viewed in the online issue, which is available at wileyonlinelibrary.com.]

were set as $W_{NL} = W_{DL} = [1\ 1]^T$ and $W_{NR} = W_{DR} = [1\ 1]$. The simulation was carried out for a total of 160 s. Step changes were made to the reference inputs at time $t = 120$ s and 140 s. Figure 17 shows the output responses of both the perturbed and the unperturbed systems using the IMC antiwindup schemes of section. Figure 18 shows the eigenvalues plot of the left-hand side of frequency-domain condition (Eq. 72) evaluated for $\forall w \in [0, \pi]$ and for a case where all the multipliers were set as unity.

Conclusions

We have demonstrated the effectiveness of the two-stage IMC antiwindup in dealing with the performance degradation associated with control windup and process directionality in input-constrained multivariable systems. The two-stage IMC antiwindup involves two low-order QPs that can be solved efficiently when compared with the intensive receding horizon control computation of MPC algorithms. We have also shown that sufficient robust stability conditions for the two-stage IMC antiwindup can be constructed via the theory of IQCs. Although we have limited our discussions to a restricted class of static IQCs for describing the plant uncertainties and input nonlinearities, stronger results may be obtained by allowing a larger class of IQCs with dynamic multipliers such as those discussed in Ref. 38. We note that the overall performance of optimizing antiwindups can be improved without necessarily trading off on robustness as demonstrated via the simulation examples.

Acknowledgments

Financial support from Petroleum Technology Development Fund (PTDF) is gratefully acknowledged.

Literature Cited

1. Campo PJ, Morari M. Robust control of processes subject to saturation nonlinearities. *Comput Chem Eng*. 1990;14:343–358.
2. Zheng A, Kothare MV, Morari M. Anti-windup design for internal model control. *Int J Control*. 1994;60:1015–1024.
3. Chen C, Perng M. An optimization-based anti-windup design for mimo control systems. *Int J Control*. 1998;69:393–418.
4. Doyle JC, Smith RS, Enns DF. *Control of plants with input saturation nonlinearities*. In: *Proceedings of the American Control Conference*. 1987:1034–1039.
5. Horla D. On directional change and anti-windup compensation in multivariable control systems. *Int J Appl Math Comput Sci*. 2009;19:281–289.
6. Tarbouriech S, Turner M. Anti-windup design: an overview of some recent advances and open problems. *IET Control Theory Appl*. 2009; 3:1–19.
7. Muske KR, Rawlings JB. Model predictive control with linear models. *AIChE J* 1993;39:262–287.
8. Rawlings JB, Chien I. Gage control of film and sheet-forming processes. *AIChE J*. 1996;42:753–766.
9. Rao CV, Rawlings JB. Steady states and constraints in model predictive control. *AIChE J*. 1999;45:1266–1278.
10. Maciejowski JM. *Predictive Control with Constraints*. Harlow, Essex: Pearson Educational Limited, 2002.
11. Soroush M, Valluri S. Optimal directionality compensation in processes with input saturation non-linearities. *Int J Control*. 1999;72: 1555–1564.
12. Edwards C, Postlethwaite I. Anti-windup and bumpless transfer schemes. *Automatica*. 1998;34:199–210.
13. Skogestad S, Morari M. *Control of ill-conditioned plants: highpurity distillation*. In: *AIChE Annual Meeting*, Miami, FL. 1986:Paper 74a.
14. Skogestad S, Morari M. Robust control of ill-conditioned plants: high-purity distillation. *IEEE Trans Automatic Control*. 1988;33: 1092–1105.
15. Pannocchia G. Robust disturbance modeling for model predictive control with application to multivariable ill-conditioned processes. *J Process Control*. 2003;13:693–701.
16. Skogestad S, Postlethwaite I. *Multivariable Feedback Control-Analysis and Design*. West Sussex: Wiley, 2005.
17. Morari M, Zafiriou E. *Robust Process Control*. Englewood Cliffs, NJ: Prentice Hall, 1989.
18. Magni L, Scattolini R. *Robustness and robust design of MPC for nonlinear discrete-time systems*. In: Findeisen R, Allgöwer F, Biegler L, editors. *Assessment and Future Directions of Nonlinear Model Predictive Control*. Heidelberg: Springer, 2007:239–254.
19. Hanus R, Kinnaert M. *Control of constrained multivariable systems using conditioning technique*. In: *Proceedings of the American Control Conference*, Pittsburgh. 1989:1711–1718.
20. Walgama KS, Sternby J. Conditioning technique for multiinput multioutput processes with input saturation. *Proc IEE Part D*. 1993: 140:231–241.
21. Peng Y, Vrančić D, Hanus R, Weller SR. Anti-windup designs for multivariable controllers. *Automatica*. 1998;34:1559–1565.
22. Kendi TA, Doyle FJ. An anti-windup scheme for multivariable nonlinear system. *J Process Control*. 1997;7:329–343.
23. Wang Y, Boyd S. Fast model predictive control using online optimization. In: 17th IFAC World Congress, Seoul. 2008:6974–6979.
24. Heath WP, Wills AG. Design of cross-directional controllers with optimal steady state performance. *Eur J Control*. 2004;10: 15–27.
25. Garcia CE, Morari M. Internal model control-1. A unifying review and some new results. *Ind Eng Chem Process Des Dev*. 1982;21: 308–323.
26. Goodwin GC, Graebe SE, Levine WS. *Internal model control of linear systems with saturating actuators*. In: *Proceedings of the European Control Conference*, Groningen. 1993:1072–1077.
27. Heath WP, Wills AG, Akkermans JAG. A sufficient condition for the stability of optimizing controllers with saturating actuators. *Int J Robust Nonlinear Control*. 2005;15:515–529.
28. Muske KR. *Steady-state target optimization in linear model predictive control*. In: *Proceedings of the American Control Conference*, Albuquerque. 1997:3597–3601.
29. Daoutidis P, Kravaris C. Structural evaluation of control configurations for multivariable nonlinear processes. *Chem Eng Sci* 1992;47: 1091–1107.
30. Soroush M, Muske KR. *Analytical model predictive control*. In: Allgöwer F, Zheng A, editors. *Nonlinear Model Predictive Control*. Switzerland: Birkhäuser Verlag Bassel, 2000:163–179.
31. Dullerud GE, Paganimi F. *A Course in Robust Control Theory: A Convex Approach*. New York: Springer-Verlag, 2000.
32. Khalil HK. *Nonlinear Systems*. Upper Saddle River, NJ: Prentice-Hall, 2000.

33. Megretski A, Rantzer A. System analysis via integral quadratic constraints. *IEEE Trans Automatic Control*. 1997;42:819–830.
34. Jönsson U, Rantzer A. *Optimization of integral quadratic constraints*. In: Ghaoui LE, Niculescu S, editors. *Advances in Linear Matrix Inequality Methods in Control: Advances in Design and Control*. Philadelphia, USA: Society for Industrial and Applied Mathematics, 2000:109–127.
35. Heath WP, Li A, Wills AG, Lennox B. *The robustness of input constrained model predictive control to infinity-norm bound model uncertainty*. In: *5th IFAC Symposium on Robust Control Design*, Toulouse, 2006.
36. Jönsson U. Lecture notes on integral quadratic constraints. Technical Report Stockholm, Department of Mathematics, KTH 2000.
37. Adegbege AA, Heath WP. *Two-stage multivariable antiwindup design for internal model control constraints*. In: *9th International Symposium on Dynamics and Control of Process Systems*, Leuven, Belgium. 2010:276–281.
38. Heath WP, Wills AG. Zames-Falb multipliers for quadratic programming. *IEEE Trans Automatic Control*. 2007;52:1948–1951.

Manuscript received Jun. 4, 2010, revision received Oct. 24, 2010, and final revision received Dec. 21, 2010.